**Online Supplemental Materials**

## 1. Materials and Methods

### A. Specific primers used for real-time RT-PCR

The specific real-time RT-PCR primers were designed and synthesized by IDT (Coralville, Iowa) and listed as follows:

Mouse MMP-3 (forward): 5'-GGA ACC TGA GAC ATC ACC AA-3'

Mouse MMP-3 (reverse): 5'-ATT CAG GCT CAG GAG TCC-3'

Mouse MMP-7 (forward): 5'-AGG AAG CTG GAG ATG TGA G-3'

Mouse MMP-7 (reverse): 5'-GCA TTT CCT TGA GGT TGT CC-3'

Mouse MMP-8 (forward): 5'-ACC CAG CAC CTA TTC ACT-3'

Mouse MMP-8 (reverse): 5'-GTA GCA TCA AAT CTC AGG TGG-3'

Mouse MMP-10 (forward): 5'-GCA TTT TGG CCC ACT CTT-3'

Mouse MMP-10 (reverse): 5'-GCC TGC TTG GAC TTC ATT-3'

Mouse MMP-13 (forward): 5'-CCC CTT CCC TAT GGT GAT-3'

Mouse MMP-13 (reverse): 5'-TCA ACT GTG GAG GTC ACT-3'

Mouse IL-1β (forward): 5'-ACG GAC CCC AAA AGA TGA AG-3'

Mouse IL-1β (reverse): 5'-TTC TCC ACA GCC ACA ATG AG-3'

Mouse IL-6 (forward): 5'-CAA AGC CAG AGT CCT TCA GAG-3'

Mouse IL-6 (reverse): 5'-GTC CTT AGC CAC TCC TTC TG-3'

Mouse IL-8 rb (forward): 5'-TCT TCC AGT TCA ACC AGC C-3'

Mouse IL-8 rb (reverse): 5'-ATC CAC CTT GAA TTC TCC CAT C-3'

Mouse TNFα (forward): 5'-GAC CCT CAC ACT CAG ATC AT-3'

Mouse TNFα (reverse): 5'-GAG ATC CAT GCC GTT GG-3'

Mouse AP-1 (forward): 5’-TTG TTA CAG AAG CAG GGA CG-3’

Mouse AP-1 (reverse): 5’-TTG CAG TCA TAG AAC GGT CC-3’

Mouse GAPDH (forward): 5’-CTT TGT CAA GCT CAT TTC CTG G-3’

Mouse GAPDH (reverse): 5’-TCT TGC TCA GTG TCC TTG C-3’

Human MMP-3 (forward): 5’-CCA GGG ATT AAT GGA GAT GCC-3’

Human MMP-3 (reverse): 5’-AGT GTT GGC TGA GTG AAA GAG-3’

Human MMP-7 (forward): 5’-TTC CAA AGT GGT CAC CTA CAG-3’

Human MMP-7 (reverse): 5’-AGT TCC CCA TAC AAC TTT CCT G-3’

Human MMP-8 (forward): 5’-GCA ACC CTA TCC AAC CTA CTG-3’

Human MMP-8 (reverse): 5’-CGA CTC TTT GTA GCT GAG GAT G-3’

Human TNFα (forward): 5’-ACT TTG GAG TGA TCG GCC-3’

Human TNFα (reverse): 5’-GCT TGA GGG TTT GCT ACA AC-3’

Human IL-1β (forward): 5’-ATG CAC CTG TAC GAT CAC TG-3’

Human IL-1β (reverse): 5’-ACA AAG GAC ATG GAG AAC ACC-3’

Human IL-6 (forward): 5’-CCA CTC ACC TCT TCA GAA CG-3’

Human IL-6 (reverse): 5’-CAT CTT TGG AAG GTT CAG GTT G-3’

Human IL-8 (forward): 5’-ATA CTC CAA ACC TTT CCA CCC-3’

Human IL-8 (reverse): 5’-TCT GCA CCC AGT TTT CCT TG-3’

Human GAPDH (forward): 5’-ACA TCG CTC AGA CAC CAT G-3’

Human GAPDH (reverse): 5’-TGT AGT TGA GGT CAA TGA AGG G-3’

**B. Biotin tracer assays on *Cldn7*$^{+/+}$ *and Cldn7*$^{-/-}$ small intestines**

1 mg/mL EZ-link™ Sulfo-NHS-LC-Biotin (Thermo Fisher Scientific, Freemont, CA; Molecular weight: 556.59) in PBS containing 1 mM $CaCl_2$ was injected into the lumen of *Cldn7*$^{+/+}$ and *Cldn7*$^{-/-}$ small intestines using a low pressure syringe pump (Harvard Apparatus, Holliston, MA) with a 25G needle connected to polyethylene tubing (PE 50, VWR International, Radnor, PA) at a rate of 50 µl/min. After 10 minutes of incubation following the biotin injection, intestines were dissected and embedded in O.C.T. compound (VWR International), then processed for immunofluorescence light microscopy. Biotin was detected by Texas red-conjugated streptavidin (Calbiochem, San Diego, CA).

## 2. Results

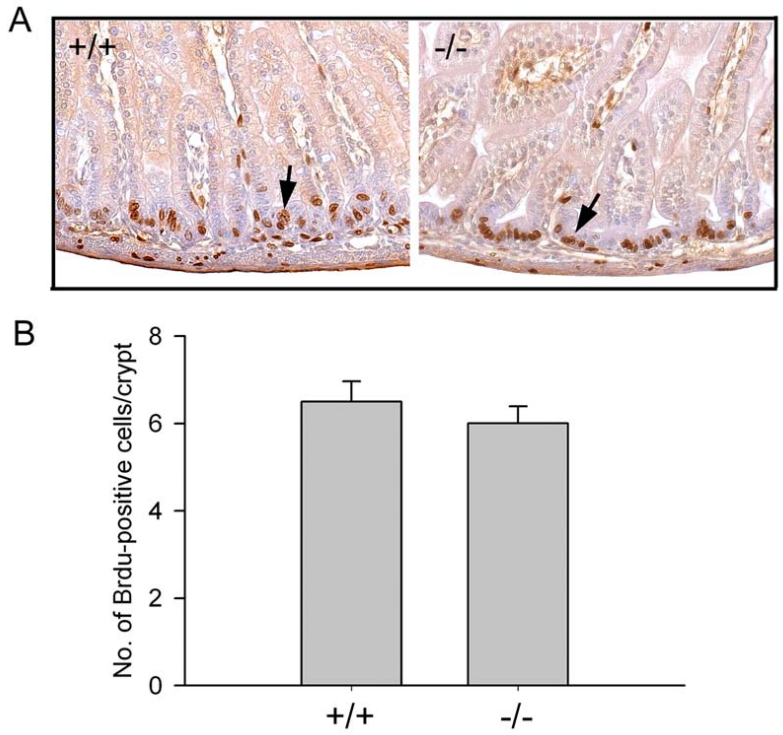


**Fig. S1** Cell proliferation in P0 (postnatal day 0) *Cldn7*$^{+/+}$ and *Cldn7*$^{-/-}$ small intestines. (A) BrdU (50mg/kg) was intraperitoneally injected into the mice. Two hours after injection, small intestines were collected and processed for immunohistochemistry. BrdU incorporation was detected by an anti-BrdU antibody as indicated by arrows. Magnification: ×600. (B) Statistical analysis showed that there was no significant difference in the number of proliferating cells in crypts between P0 *Cldn7*$^{+/+}$ and *Cldn7*$^{-/-}$ small intestines. Data was obtained from three independent samples.

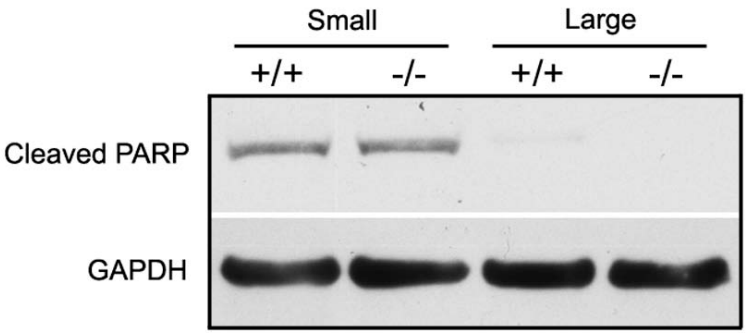


**Fig. S2** Expression of cleaved PARP in P0 *Cldn7*$^{+/+}$ and *Cldn7*$^{-/-}$ intestines. Cleaved PARP served as a marker for apoptosis. Western blotting showed that there was no significant change of cleaved PARP expression between *Cldn7*$^{+/+}$ and *Cldn7*$^{-/-}$ small intestines. Anti-cleaved PARP signal was barely detected in large intestines. GAPDH was used as a protein loading control.

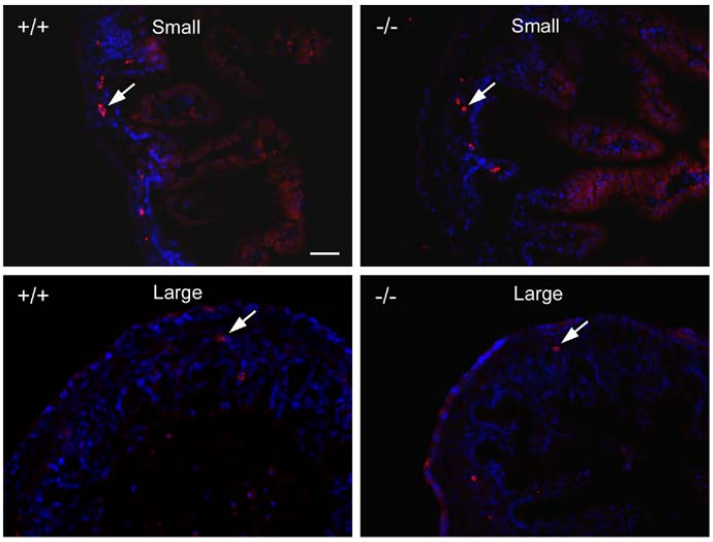


**Fig. S3** Frozen sections of small and large intestines from P0 *Cldn7*$^{+/+}$ and *Cldn7*$^{-/-}$ mice were stained using an antibody recognizing macrophages (red) as indicated by arrows. Nuclei were stained blue. There was no significant change in the number of macrophages between *Cldn7*$^{+/+}$ and *Cldn7*$^{-/-}$ sections. Bar: 20 μm.

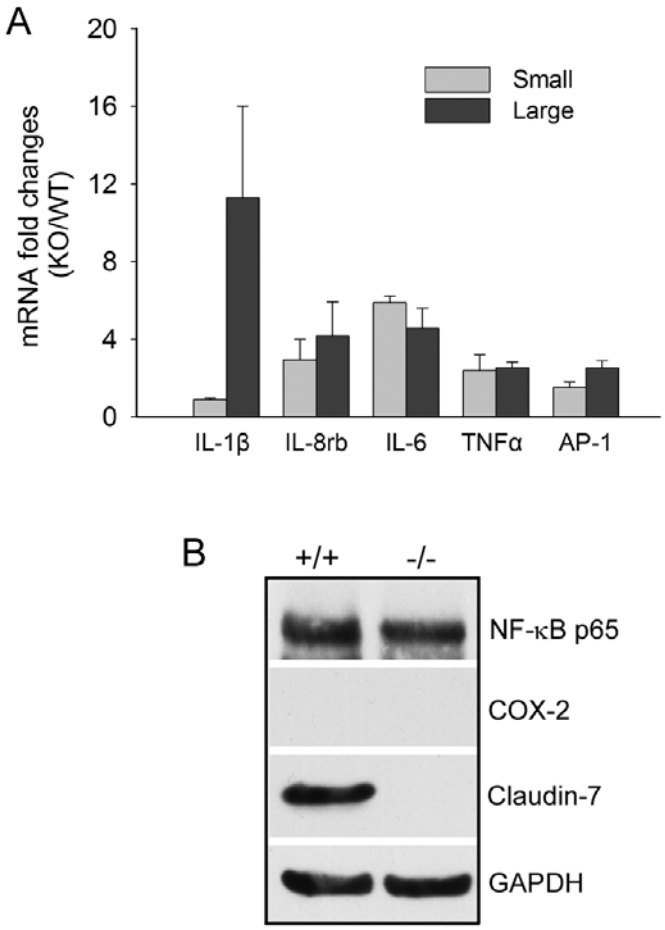


**Fig. S4** Cytokine mRNA levels and NF-κB expression in P0 *Cldn7*$^{+/+}$ and *Cldn7*$^{-/-}$ intestines. (A) Each specific mRNA value was normalized to its GAPDH mRNA level. The mRNA fold changes were calculated after comparing *Cldn7*$^{-/-}$ values to those of *Cldn7*$^{+/+}$. The IL-1β mRNA level measured by qRT-PCR was significantly increased in *Cldn7*$^{-/-}$ large intestine. Each data point was obtained from five independent experiments. (B) Western blotting showed no significant change of NF-κB p65 expression in P0 *Cldn7*$^{-/-}$ small intestines compared to that in *Cldn7*$^{+/+}$. There was no detectable signal of COX-2 in both *Cldn7*$^{+/+}$and *Cldn7*$^{-/-}$ small intestines. These results were consistent with the histological observation that inflammation was not initiated in P0 *Cldn7*$^{-/-}$ intestines.

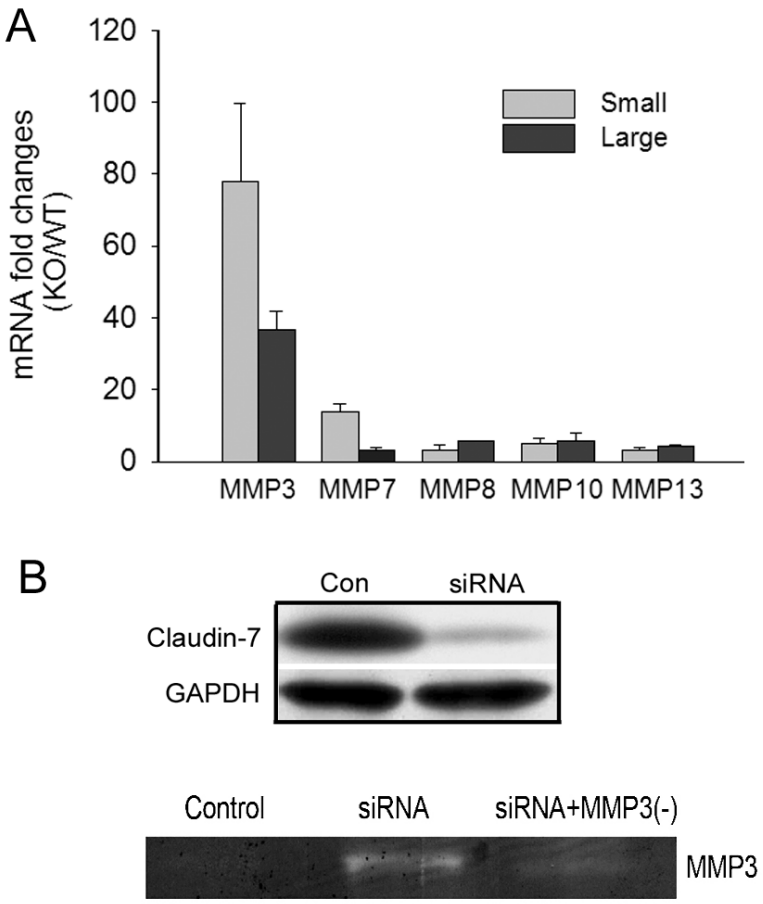


**Fig. S5** (A) MMP-3 mRNA level measured by qRT-PCR was greatly increased in P0 *Cldn7*$^{-/-}$ small and large intestines. Fold changes were calculated using the same method as described in Fig. S4 A. Each data point was obtained from five independent experiments. (B) Inhibition of MMP-3 activity in T84 cells. Claudin-7 was transiently knocked down in T84 cells using specific siRNA against claudin-7 (top). MMP-3 inhibitor II (Calbiochem) was added to the culture medium overnight. The medium was collected, centrifuged, and concentrated for casein zymography gel analysis. Results showed the increased enzymatic activity of MMP-3 in claudin-7 knockdown cells, and this increase was inhibited after adding MMP-3 inhibitor (-) to the medium.

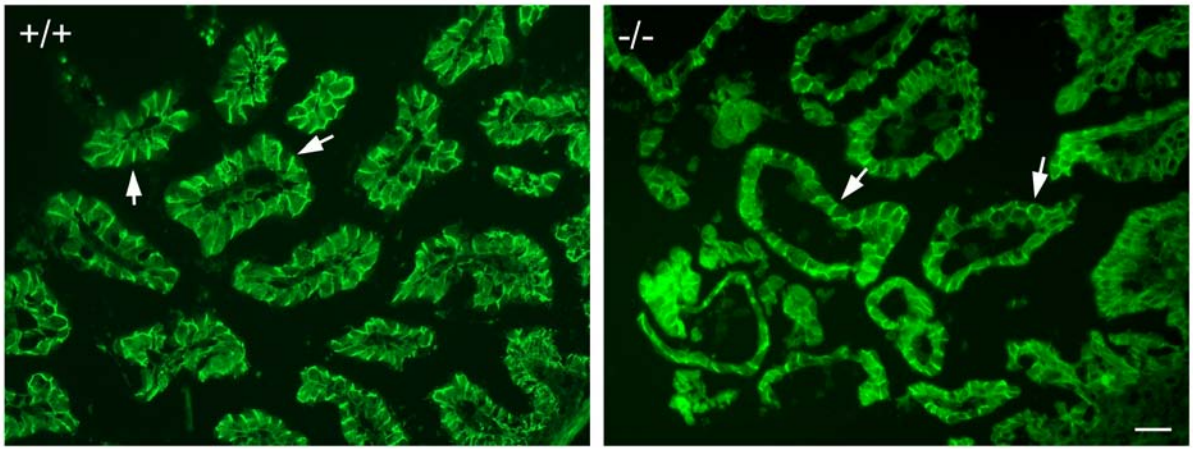


**Fig. S6** Localization of Na-K ATPase in *Cldn7*$^{+/+}$ and *Cldn7*$^{-/-}$ small intestines. Frozen sections of P4 *Cldn7*$^{+/+}$ and *Cldn7*$^{-/-}$ small intestines were immunostained with the primary antibody against Na-K ATPase α1 subunit. The arrows indicated the basolateral localization of Na-K ATPase in *Cldn7*$^{+/+}$ (+/+) and *Cldn7*$^{-/-}$ (-/-) small intestines. Bar: 20 μm.

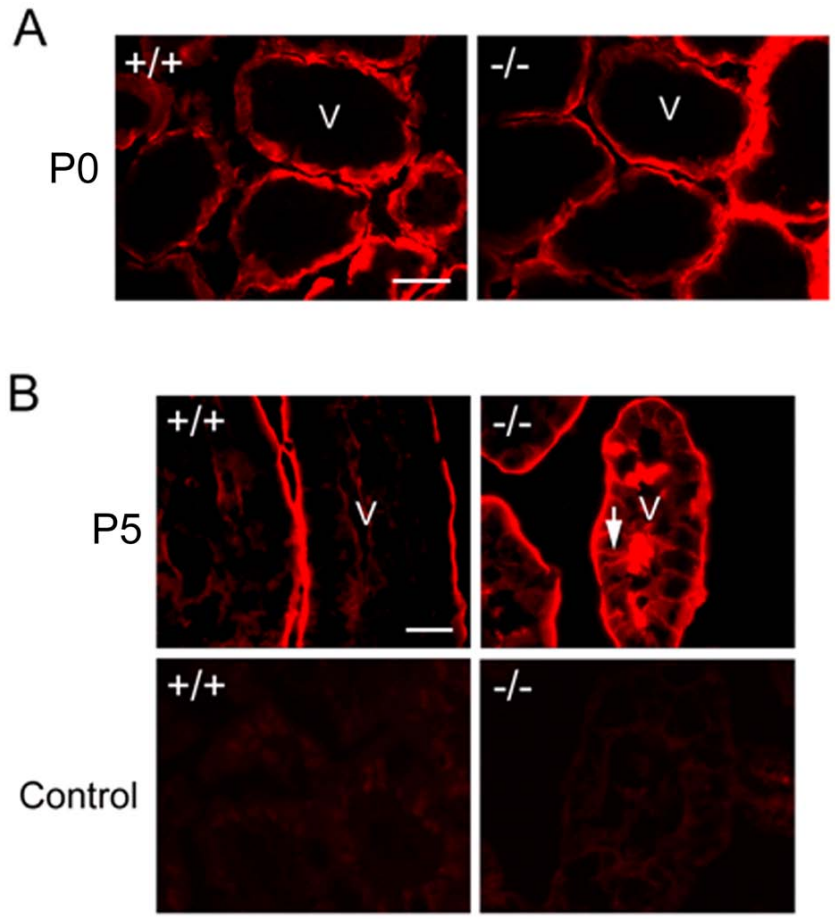


**Fig. S7** Biotin tracer assays in *Cldn7*$^{+/+}$ and *Cldn7*$^{-/-}$ small intestines. Sulfo-NHS-LC-Biotin was injected into the P0 (A) or P5 (B) intestinal lumen, and then stained with Texas red-conjugated streptavidin. No barrier leakage was detected in P0 *Cldn7*$^{+/+}$ and *Cldn7*$^{-/-}$ small intestines. In contrast, the leakage was detected in P5 *Cldn7*$^{-/-}$ small intestines (B, arrow in -/-). Intestines without biotin injection were used as negative controls. V: Villus; Bars: 20 μm.

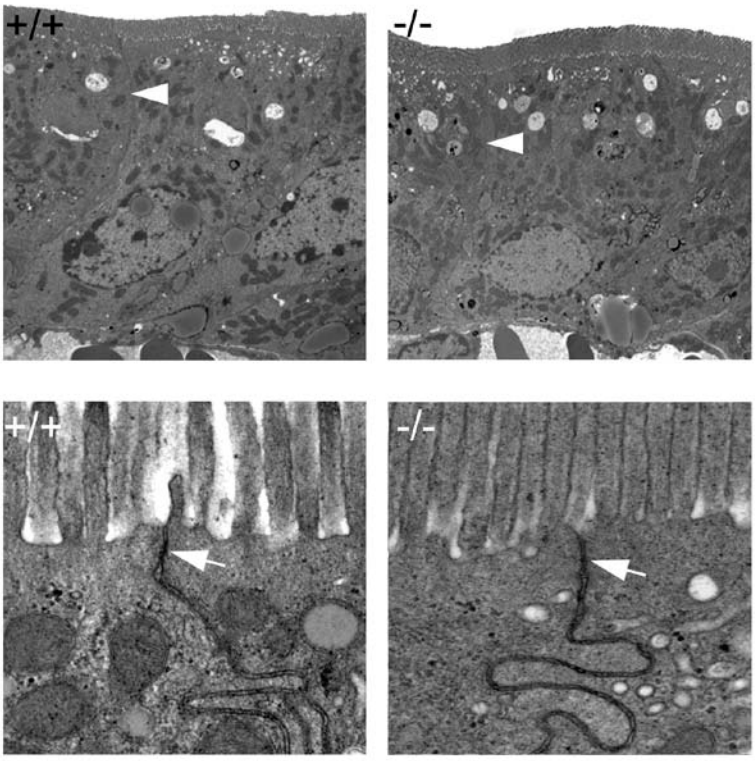


**Fig. S8.** Electron micrographs of P0 *Cldn7*$^{+/+}$ (+/+) and *Cldn7*$^{-/-}$ (-/-) small intestines. The arrowheads in the upper panel point to the intact cell-cell connection between two adjacent epithelial cells. The arrows in the bottom panel indicate the TJ structure in *Cldn7*$^{+/+}$ (+/+) and *Cldn7*$^{-/-}$ (-/-) small intestines. Magnifications: upper panel: ×5,000; lower panel: ×50,000.

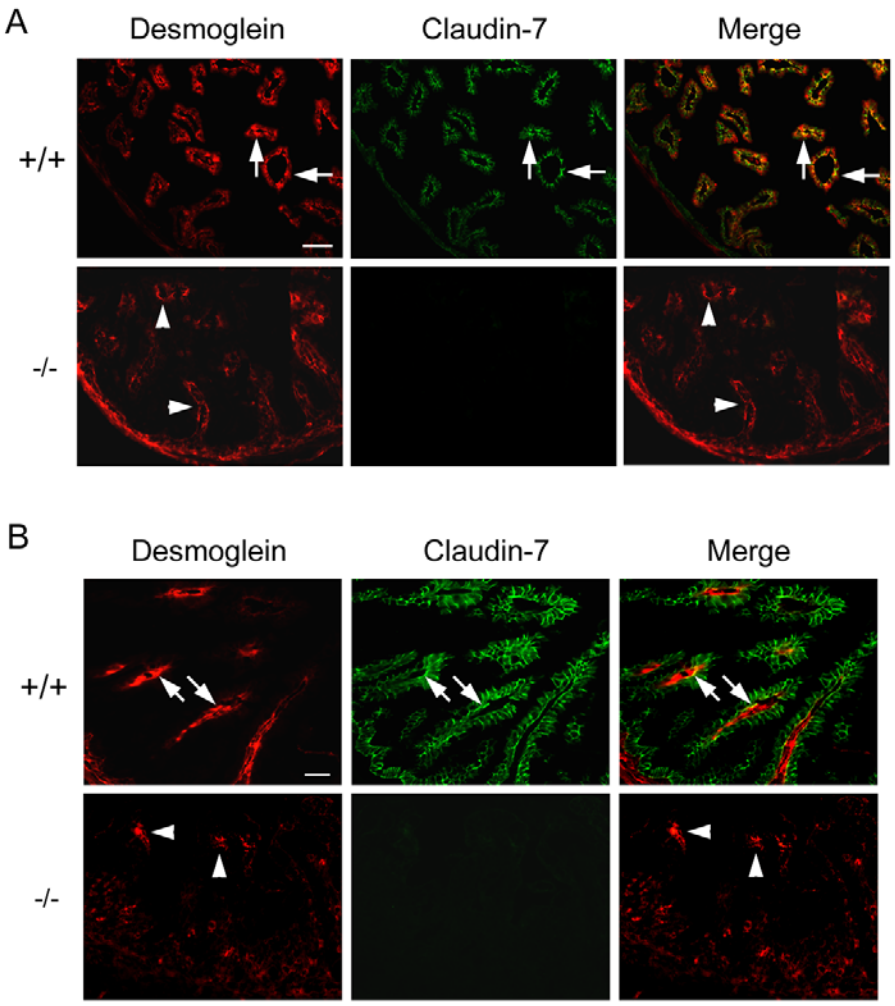


**Fig. S9** Desmoglein localization in P0 (A) and P5 (B) *Cldn7*$^{+/+}$ and *Cldn7*$^{-/-}$ small intestines. The double immunofluorescent staining showed the partial co-localization of desmoglein with claudin-7 at the basolateral membrane of *Cldn7*$^{+/+}$ intestines (A and B, arrows in +/+). However, the localization of desmoglein was disrupted and disorganized in P5 *Cldn7*$^{-/-}$ small intestines as indicated by the arrowheads (B, -/-). Bars: 40 µm.

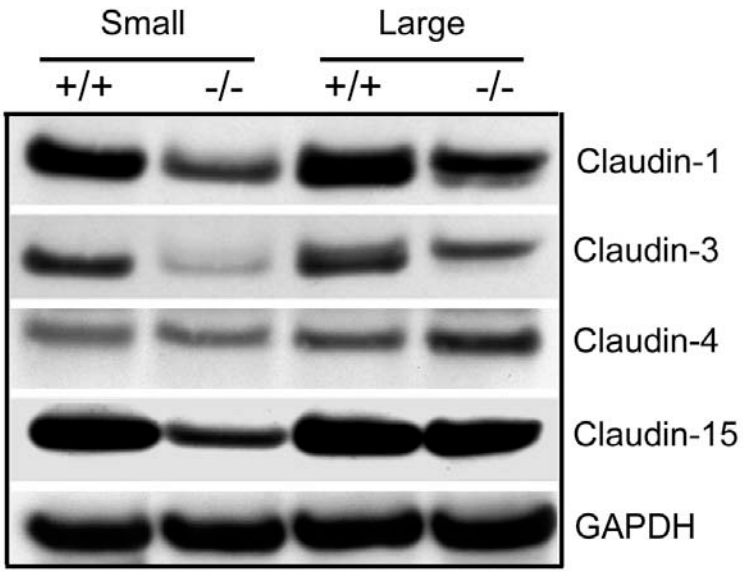


**Fig. S10** Expression of claudin proteins in P5 *Cldn7*$^{+/+}$ and *Cldn7*$^{-/-}$ intestines. Western blotting showed that the expression levels of claudin-1 and claudin-3 were significantly decreased in both small and large *Cldn7*$^{-/-}$ intestines when compared to those of *Cldn7*$^{+/+}$. No significant change in claudin-4 expression between *Cldn7*$^{+/+}$ and *Cldn7*$^{-/-}$ intestines. Claudin-15 was significantly decreased in *Cldn7*$^{-/-}$ small intestines but not in large intestines. GAPDH was used as a protein loading control.